

Hydrogeomorphic response of steep streams following severe wildfire in the Western Cascades, Oregon

David M. Busby | Andrew C. Wilcox 

Department of Geosciences, 32 Campus Drive, University of Montana, Missoula, Montana, USA

Correspondence

Andrew C. Wilcox, Department of Geosciences, 32 Campus Drive, University of Montana, Missoula, MT 59812, USA.
 Email: andrew.wilcox@umontana.edu

Funding information

National Science Foundation, Grant/Award Numbers: EAR1644619, DGE 1633831; North Umpqua Foundation; Geological Society of America Graduate Research Grant

Abstract

Severe wildfire may alter steep mountain streams by increasing peak discharges, elevating sediment and wood inputs into channels, and increasing susceptibility to landslides and debris flows. In the Pacific Northwest, where mean annual precipitation is high and mean fire-return intervals range from decades to centuries, understanding of steep stream response to fire is limited. We evaluate the hydrologic and geomorphic response of ~100-m-long steep stream reaches to the large-scale and severe 2020 fires in the Western Cascade Range, Oregon. In the two runoff seasons after the fires, peak flows in burned reaches were below the 2-year recurrence interval flood, a level sufficient to mobilize the median grain size of bed material, but not large enough to mobilize coarser material and reorganize channel morphology. Sediment inputs to study streams consisted of two road-fill failure landslides, slumps, sheetwash, and minor bank erosion; precipitation thresholds to trigger debris flows were not exceeded in our sites. There was a 50% increase in the number of large wood pieces in burned reaches after the fires. Changes in fluxes of water, sediment, and wood induced shifts in the balance of sediment supply to transport capacity, initiating a sequence of sediment aggradation and bed-material fining followed by erosion and bed-material coarsening. Gross channel form showed resilience to change, and an unburned reference reach exhibited little morphologic change. Post-fire recruitment of large wood will likely have long-term implications for channel morphology and habitat heterogeneity. Below-average precipitation during the study period, combined with an absence of extreme precipitation events, was an important control on channel responses. Climate change may have a complex effect on stream response to wildfire by increasing the propensity for both drought and extreme rain events and by altering vegetation recovery patterns.

KEY WORDS

burn severity, landslides, post-fire, resilience, step-pool, surface erosion, thresholds

1 | INTRODUCTION

Severe fire alters soil, vegetation, and hydrologic properties of mountain watersheds, commonly elevating inputs of water, sediment, and wood to channel networks and potentially altering the form and function of steep mountain streams (e.g. Benda, Miller et al., 2003; Shakesby & Doerr, 2006). Post-fire floods, hillslope erosion processes (e.g. Shakesby & Doerr, 2006), and associated geomorphic changes can threaten infrastructure, homes, and lives (Jakob & Hungr, 2005; Kean et al., 2019) and disturb aquatic ecosystems (Florsheim,

O'Dowd, & Chin, 2024). The hydrogeomorphic responses of mountain streams to wildfire have been well studied in semiarid regions of the western United States, where mean fire return intervals are years to decades (e.g. Chin et al., 2019; Hoffman & Gabet, 2007; Minshall, Robinson, & Lawrence, 1997; Rengers et al., 2020; Thomas et al., 2023). In the temperate Pacific Northwest, however, where fire return intervals range from decades to centuries but high precipitation and prevalent steep topography create susceptibility to post-fire flooding and mass wasting processes (e.g. landslides and debris flows; McNabb & Swanson, 1990; Wondzell & King, 2003;

Jackson & Roering, 2009), understanding of post-fire stream response is limited.

In early September 2020, several extensive, high-severity wild fires ignited across the Western Cascade Range, Oregon. In what are collectively known as the Labor Day fires, more area burned in the Oregon Cascades than in the previous five decades combined (Reilly et al., 2022), likely exceeding annual burned area since at least 1900 (Abatzoglou et al., 2021). The fires, at least some of which were human-related ignitions associated with power lines (Sickinger, 2022), were enabled by extreme fuel aridity and driven by a strong east wind event (Abatzoglou et al., 2021). The historic magnitude and severity of the 2020 fires in the Western Cascades create impetus to investigate post-fire landscape responses. Evidence of shifts in fire regimes across the Pacific Northwest (Haugo et al., 2019) and projections of climate-change-induced increases in fire weather (Jones et al., 2022), fire activity (e.g. Halofsky, Peterson, & Harvey, 2020; Littell et al., 2018), and post-wildfire extreme rainfall (Touma et al., 2022) in the region provide further motivation.

Several studies of the 2020 western Oregon fires have been completed (e.g. Calhoun et al., 2022; Coble et al., 2023; Moffett & Quinn, 2023; Roebuck et al., 2022). Metrics characterizing fine sediment content or large wood did not show significant differences in the year after the fires among streams that experienced different fire severities (Coble et al., 2023), but dissolved organic-matter composition did show differences in post-fire response depending on burn severity (Roebuck et al., 2022). Higher soil-moisture content in the top several centimetres reduced hydrophobicity in several areas burned in the Labor Day fires, especially in clay loam and silt loam soils; hydrophobicity also varied with residual organic content (Moffett & Quinn, 2023). Calhoun et al. (2022) found that some debris flows, shallow landslides, rockfall, and instances of flood scour were evident in areas that burned in 2020, but most of the drainages surveyed did not experience post-fire mass wasting events in the two winters after the fires. Our study complements these efforts by investigating the hydrogeomorphic response of mountain streams to the 2020 Oregon fires.

The bed and bank structure of steep mountain streams fosters resilience to moderate changes in discharge and sediment inputs following disturbance (e.g. Chin, 1989; Montgomery & Buffington, 1998). Boulders deposited in channels (Grant, Swanson, & Wolman, 1990) create keystones that form stable bed structures, including steps, grain clusters and grain nets (Church, 2006; Comiti & Mao, 2012; Grant, Swanson, & Wolman, 1990). The morphologic resilience of steep streams may change following severe fire, however, as a result of changes to soil, vegetation, and hydrologic properties of mountain watersheds and resulting alteration of water, sediment, and wood fluxes. Fire-induced removal of vegetation and litter exposes soil to raindrop impact, reduces surface storage capacity, and increases susceptibility to overland flow and hillslope erosion processes, including dry ravel, sheetwash, riling, gullying, landslides, and debris flows (e.g. Hyde et al., 2016; Robichaud, 2000; Roering & Gerber, 2005). Increased soil water repellency (i.e., hydrophobicity) can also reduce infiltration but may be highly localized and spatially variable (McGuire et al., 2018; Shakesby & Doerr, 2006). Wood supply to mountain streams can be amplified following fire as a result of accelerated treefall and bank erosion (e.g. Benda et al., 2003; Minshall, Robinson, & Lawrence, 1997).

Fire-induced changes to hillslope processes and hydrogeomorphic fluxes can lead to variable and in some cases dramatic changes to channel morphology. Landslides and debris flows can reorganize steep mountain streams by scouring channels to bedrock and/or supplying wood and sediment, which aggrades channel beds and produces debris fans that restrict channel width and alter upstream and downstream morphology (e.g. Benda, 1990; Benda, Veldhuisen, & Black, 2003; Germanoski & Miller, 1995; Hoffman & Gabet, 2007; May & Gresswell, 2004). Depending on the timing and intensity of post-fire precipitation, post-fire mass-wasting may be delayed several years, until after root systems decay and associated cohesion is lost, and before new vegetation and root systems are established (Jackson & Roering, 2009; Rengers et al., 2020; Roering et al., 2003). Surface erosion processes, including dry ravel and riling, can input enough sediment to steep streams to bury steps and pools (e.g. Florsheim et al., 2017; Florsheim, Keller, & Best, 1991; Keller, Valentine, & Gibbs, 1997). By increasing flow resistance and reducing sediment transport capacity (e.g. Montgomery et al., 2003), large wood jams can cause further aggradation of post-fire sediment inputs (Chin et al., 2024; Rengers et al., 2023; Short, Gabet, & Hoffman, 2015; Wohl et al., 2022).

Post-fire-hydrogeomorphic responses are highly variable across regions and watersheds due to interacting climatic, biophysiological, and anthropogenic factors (e.g. Benda & Dunne, 1997; Florsheim, O'Dowd, & Chin, 2024; Moody et al., 2013; Shakesby & Doerr, 2006). Influential factors include burn severity and extent, precipitation (magnitude, duration, intensity), dominant runoff mechanisms (e.g., overland versus subsurface flow), channel and basin morphology (e.g., gradient, confinement), vegetation (type, coverage, rate of regrowth), soils (type, thickness), lithology, and land management (e.g., timber harvest, road construction) (Swanson, 1981; Sidle, Pearce, & O'Loughlin, 1985; McNabb & Swanson, 1990; Montgomery & Buffington, 1998; Cerda & Doerr, 2005; Shakesby & Doerr, 2006; Moody et al., 2013; Vieira et al., 2015; Ebel et al., 2023; Figure 1).

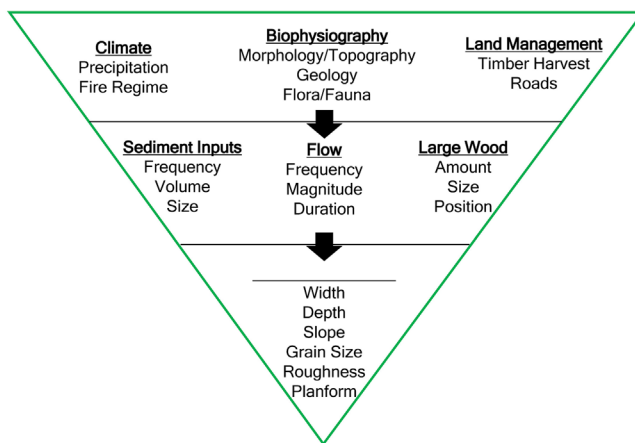


FIGURE 1 Conceptualization of the tiered controls on steep stream morphology. Wildfire influences steep-stream morphology via its effect on sediment, flow, and wood regimes. Specific attributes of the fire regime (e.g. burn severity), post-fire precipitation (timing, magnitude, and intensity), biophysiology (e.g., vegetation regeneration rates, hillslope gradient), and human interventions will govern the extent to which the balance of sediment supply and transport capacity shifts following wildfire, and in turn the potential for geomorphic adjustments.

The objective of this study was to evaluate the hydrologic and geomorphic response of steep streams to severe wildfire in the Western Cascades. We measured streamflow, instream wood, and post-fire changes in channel topography and bed-material size in four steep stream reaches that burned in the 2020 wildfires, and we compared observations to conditions in an unburned reference reach and nearby gaged streams. We assessed post-fire precipitation, sediment inputs, and flow competence to contextualize hydrogeomorphic responses. Further, we interpreted channel responses in the context of variable biophysiographic site characteristics (Figure 1) to provide insight on the potential controls on post-fire geomorphic responses. This work advances understanding of watershed response to high-severity fire in a region that is increasingly susceptible to climatic disturbance (e.g., wildfire, drought, intense rainstorms) and has implications for post-fire hazard mitigation and management.

2 | STUDY AREA

We investigated four steep stream reaches in watersheds burned in the 2020 Archie Creek and Holiday Farm fires in the Western Cascades of Oregon (Figure 2). These fires burned over 1200 km², 74% of which was at moderate or high soil burn severity (U.S. Geological Survey) & (U.S. Forest Service, 2020). The area in which the Archie Creek Fire burned is characterized as having a mixed and stand-replacement severity fire regime, with mean fire-return intervals of 35–200 years (U.S. Geological Survey, 2022a). The Holiday Farm Fire burn area has a stand-replacement severity fire regime, with return intervals of greater than 200 years (U.S. Geological Survey, 2022a).

The Western Cascade Range flanks the western slope of the Oregon Cascades and comprises a Miocene-upper Eocene volcanic arc, with dacitic tuffs, andesite lava flows, and lesser basaltic and rhyolitic volcanic rocks (Conrey et al., 2002). Hillslope dissection is driven by glacial erosion, streams fed by shallow subsurface stormflow, and debris flows, producing a landscape with steep slopes and extensive drainages (Jefferson et al., 2010). Relatively high rates of runoff and erosion provide substantial bed material to rivers (Jefferson et al., 2010; O'Connor et al., 2014; Swanson, 1975). Both the Archie Creek and Holiday Farm fires straddled the boundary of the foothills and the steeper, high-relief interior of the Cascades and engulfed large east–west lying rivers, the North Umpqua River and McKenzie River, respectively, both of which are important regional rivers for water supply and salmon fisheries. Tributary streams flow north and south linking steep ridges with the gentler McKenzie River and North Umpqua River valleys.

We selected study reaches that we expected, on the one hand, to be resilient to disturbance because of high transport capacities, coarse bed materials, and stable bed structures; but on the other hand, to have high propensity for geomorphic change from post-fire runoff and erosion based on their basin attributes. As such, study basins have predominantly steep gradients (mean basin slopes 30%–56%) and experienced moderate or high soil burn severity (between 61% and 99% of basin area) during the 2020 fires (Figure 2; Table 1), meaning that nearly all the organic ground cover was consumed by fire. Study reaches (Figure 2, Table 1) are in third- and fourth-order streams, in the vicinity of junctions with headwater tributaries, corresponding to locations in the stream network more frequently

subject to landslide and debris-flow deposits (e.g. Benda, Veldhuisen, & Black, 2003; Bigelow et al., 2007). Study reaches are also within or near channel segments predicted by the US Geological Survey to have high debris-flow hazard in response to a 15-min, 24 mm h⁻¹ rainfall intensity (U.S. Geological Survey, 2020). Study reaches are steep (~5%–10% gradients; Table 1), coarse (predominantly cobble- and boulder-bedded), and exhibit step-pool and step-riffle (intermediate between step-pool and pool-riffle) morphologies.

Wright Creek (WRT), Bogus Creek (BOG), and Swamp Creek (SWP) burned in the Archie Creek Fire and are tributaries of the North Umpqua River. Cone Creek (CON) burned in the Holiday Farm Fire and is a tributary of the McKenzie River. Hillslopes adjacent to study reaches in WRT and CON are dissected by steep gullies rated with high and moderate debris-flow hazard, respectively. A perennial tributary with high debris-flow hazard enters SWP (U.S. Geological Survey, 2020). At the onset of this study in late 2020, following the fires, selection of burned study reaches was constrained by accessibility and safety concerns. We also have one unburned reference reach, McRae Creek (MCR), to enable comparison of post-fire responses between burned and unburned sites. MCR is 8 km northwest of the Holiday Farm Fire, in the HJ Andrews Experimental Forest (Figure 2), and is a National Ecological Observation Network (NEON) site with continuous records of stage and discharge and pre-fire channel morphology data.

Prior to the 2020 fires, forested areas were dominated by Douglas-fir (*Pseudotsuga menziesii*) and western hemlock (*Tsuga heterophylla*; (U.S. Geological Survey, 2022a). All study basins have experienced timber harvest, primarily via stand clearcutting, and associated road construction (Table 1). Only BOG has been harvested since 1998, as part of a small salvage logging operation following the 2009 Williams Creek Fire, which burned nearly all of the catchment at mixed severity (U.S. Forest Service), 2022; (U.S. Geological Survey) & (U.S. Forest Service), 2022. Thirty percent of WRT burned at low severity in 2017 (U.S. Geological Survey) & (U.S. Forest Service), 2020.

Mean annual precipitation in study basins ranges from ~1.5 to 2.2 m (PRISM Climate Group, 2022; Table 1). Most precipitation occurs during the winter as rain during long-duration, low-intensity frontal storms, with mixed rain and snow above ~600 m in elevation. All study reaches other than MCR are lower elevation (Table 1) and are thus rainfall-dominated. Summers are relatively warm and dry. Characteristic organic matter-rich loam soils have a high infiltration capacity.

3 | METHODS

3.1 | Field surveys

To measure post-fire hydrogeomorphic responses, we conducted repeat field surveys in the 1.5 years after the wildfires, encompassing two winters, when most precipitation occurs in the study area. We were first able to access the burned areas in mid-December 2020, 1.5 months after the fires were contained, and about 3 months after most of the fire spread. This was following a mid-November 24-h, 76 mm (USGS Cougar Dam Met Station #440752122143200, elevation 383 m; Figure 2) and 58 mm (Archie1 tipping-bucket gage,

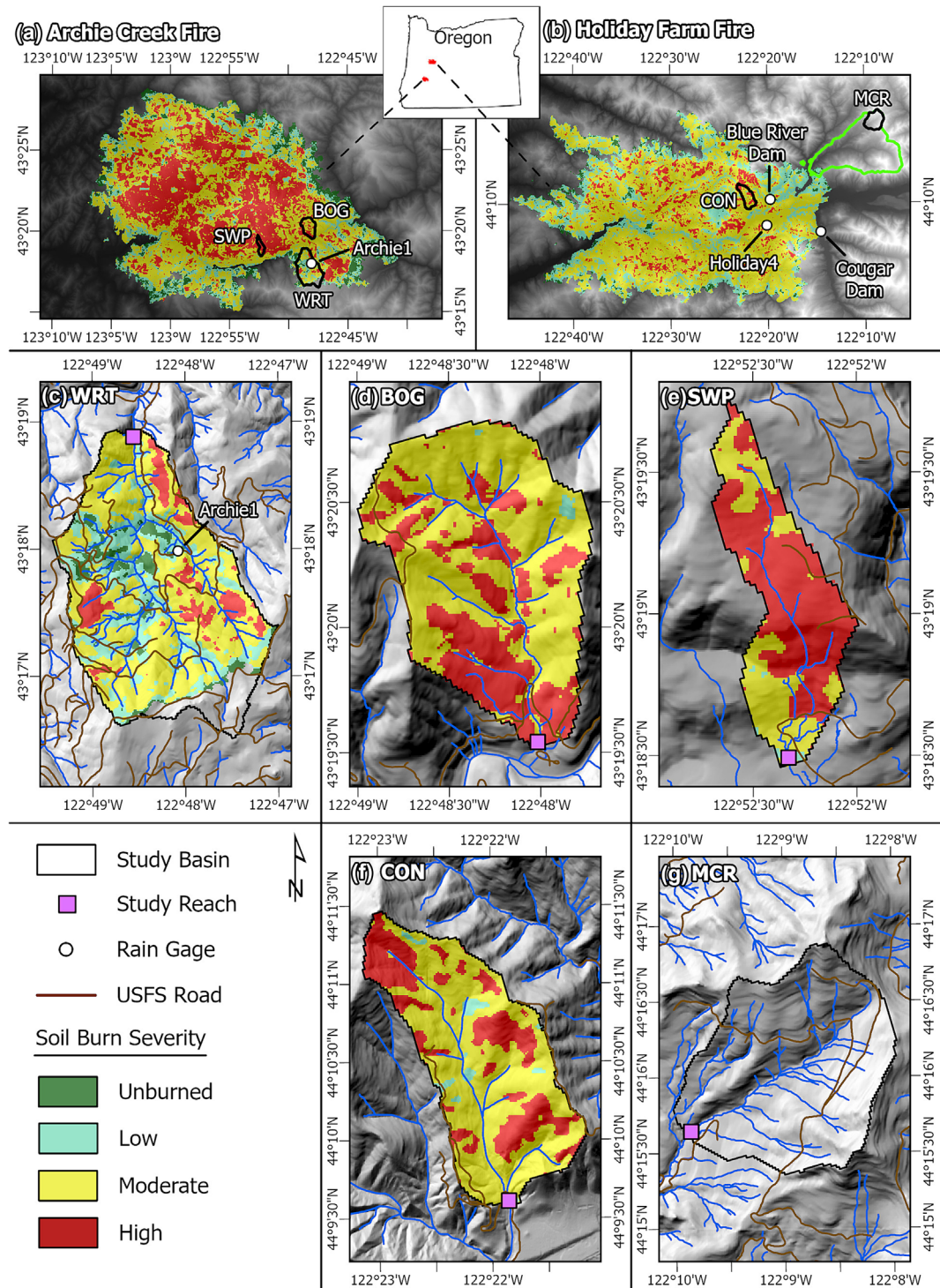


FIGURE 2 Study area maps, including study basin outlines, reach locations, rain gages used in this analysis, and burn severity of (a) Archie Creek and (b) Holiday Farm fires, with labelled study basin locations; (b) also shows HJ Andrews Experimental Forest (green polygon); (c) Wright Creek (WRT), (d) Bogus Creek (BOG), (e) Swamp Creek (SWP), and (f) Cone Creek (CON) study basins. (g) Shows hillshade and channel network of unburned MCR basin. MCR, McRae Creek.

elevation 619 m; Figure 2) rain event near the Holiday Farm Fire study sites (reach elevations 352–884 m; Table 1) and Archie Creek Fire study sites (reach elevations 306–410 m; Table 1), respectively. Some post-fire geomorphic changes may therefore have occurred by the time of initial field surveys. We conducted repeat surveys of burned reaches in June 2021 and March 2022. We surveyed the unburned reference reach, MCR, in June 2021 only, otherwise relying on NEON data for MCR.

During each field visit, we used a Leica TS06 total station and an Emlid Reach GPS receiver to conduct georeferenced surveys of 5–11 cross sections per reach and thalweg longitudinal profiles. To characterize grain size of the mobile clasts, we completed a Wolman pebble count of ~100 grains, excluding boulders (Wolman, 1954), in each reach, in a location representative of the bed material. We measured discharge during each field visit along a cross section with relatively simple geometry using a SonTek FlowTracker ADV. We installed an

TABLE 1 Characteristics of Wright Creek (WRT), Bogus Creek (BOG), Swamp Creek (SWP), Cone Creek (CON), and McRae Creek (MCR) study sites.

	WRT	BOG	SWP	CON	MCR
Fire	Archie	Archie	Archie	Holiday	N/A
Reach slope (%)	4.8	6.0	10.0	5.9	6.2
Reach length (m)	71	116	116	107	53
Mean reach elevation ^a (m)	328	306	410	352	884
Drainage area ^a (km ²)	8.9	2.8	1.1	4.5	4.2
Mean basin slope ^a (%)	45	56	30	51	39
Basin relief ^a (m)	1010	628	622	945	713
Harvested area ^b (%)	48	1	27	0	21
Pre-fire forested area ^c (%)	100	59	79	100	100
Road density (km km ⁻²) ^d	2.4	1.0	1.2	0.7	1.6
Mean annual precipitation ^e (m)	1.6	1.5	2.0	2.1	2.2
% High burn severity ^f	9	34	64	30	0
% Moderate burn severity ^f	52	65	35	68	0
% Low burn severity ^f	24	1	1	3	0
% Unburned ^f	14	0	0	0	100

Abbreviation: USFS, U.S. Forest Service.

^aU.S. Geological Survey (2022b).

^bPercent of catchment area that has been harvested in the past; may not include all historic harvest activity U.S. Forest Service, 2022).

^cU.S. Geological Survey (2022a).

^dU.S. Forest Service (2022).

^eTotal of rain and snow water equivalent (PRISM Climate Group, 2022).

^fSoil burn severity of study basin as percent of total area (U.S. Geological Survey) & (U.S. Forest Service), 2020).

In-Situ Level TROLL 300 pressure transducer in each ungauged reach to record stage at 15-min intervals, and barometric pressure transducers adjacent to WRT and CON to correct for atmospheric pressure. To provide visual documentation of variability in daily stream conditions (stage and turbidity), Browning Recon Force trail cameras were mounted to tree trunks and directed at streams, large wood jams, and gullies. Cameras took two photos per day. MCR has a permanent trail camera that takes a photo every 30 min during daylight. Finally, we photographed the length of study reaches to document changes in stream morphology, large wood, and point sources of sediment (e.g., slumps, bank erosion).

To further characterize stream and hillslope conditions and erosion processes, we conducted uncrewed aerial vehicle (UAV) surveys (collecting RGB photos and video) of study reaches and upstream catchment areas. UAV surveys were completed from a height of ~100 m, and photos were processed into four-cm resolution, georeferenced orthophotos in Pix 4D Mapper. The UAV surveys provided a means to identify large sediment sources such as landslides, over a broader spatial scale than ground surveys, but they do not provide a complete representation of all surface-erosion mechanisms, such as sheetwash, small rills, or dry ravel. We estimated landslide and debris fan volumes using UAV imagery-derived digital surface models (DSMs) in Pix4D, by digitizing the volume base (i.e., the footprint of the landslide scar or debris fan) and calculating the volume between the base and the surface defined by the DSM. The first UAV survey, of BOG basin, was completed by the University of Washington Natural Hazards Reconnaissance (RAPID) Facility in March 2021. We conducted additional UAV surveys of burned sites in June 2021 and March 2022 using a DJI Mavic 2 Pro.

3.2 | Precipitation and hydrologic response

To quantify precipitation, we used data from tipping-bucket rain gages installed by research collaborators, USGS meteorological stations, and the PRISM Climate Group. The tipping-bucket gages, one of which (Archie1) was in the WRT basin, the other of which (Holiday4) was 3 km from CON, were in place from November 2020 to September 2021. For water years (WYs) 2021 and 2022, we determined total precipitation, percent of normal precipitation, and Z-scores of total precipitation, which are calculated as the number of standard deviations away from the mean. We also calculated maximum daily precipitation and maximum 24-h precipitation, the latter of which has been used to characterize debris flow thresholds in western Oregon (Wiley, 2000). Finally, we calculated the maximum 15-min rainfall intensity, a metric used by the USGS to characterize debris flow hazard (U.S. Geological Survey), 2020.

To evaluate hydrologic response to the 2020 wildfires, we assessed peak flow stage (measured with pressure transducers), discharge, and the duration of flows exceeding the level we identified as bankfull, based on morphologic and vegetation indicators. We modelled hydraulic conditions using HEC-RAS (Hydrologic Engineering Center's River Analysis System). HEC-RAS requires cross-section geometries, Manning's *n*, and discharge, and outputs a water surface elevation (WSE) profile and cross section-averaged hydraulic metrics (e.g., velocity, shear stress) at each cross section for the modelled flow. For topography input, we used cross sections measured during March 2022 field surveys. We calibrated the Manning's *n* roughness coefficient by simulating field discharges from December 2020 and March 2022 and fitting modelled WSE to field-

measured WSEs. To estimate peak flows, we varied discharge in HEC-RAS until the modelled WSE matched the WSE recorded by pressure transducers during the peak flows in 2021 and 2022 (additional details on HEC-RAS modeling are provided in Busby, 2022). We compared timing, magnitude, and recurrence intervals (estimated using USGS regression relations; (U.S. Geological Survey), 2022b) of peak discharges in study streams to those in both burned and unburned gaged creeks in HJ Andrews Experimental Forest and nearby USGS gaged streams.

3.3 | Geomorphic response

To evaluate the geomorphic response of steep streams to the 2020 wildfires, we measured changes in channel topography and bed-material size. In burned study reaches (WRT, BOG, SWP, CON), we calculated changes between each field survey and over the entire study period. As such, change was measured for three time periods: December 2020 to June 2021, June 2021 to March 2022, and December 2020 to March 2022. From cross-section data, we calculated the percent change in reach-averaged bankfull width and depth during each time period and tested for significant differences using the nonparametric Wilcoxon rank sum test, which is applicable to small sample sizes and nonnormally distributed data. We evaluated changes in thalweg longitudinal profiles by calculating the change in reach slope and bed roughness height, as characterized by the standard deviation of the thalweg elevation (Coleman, Nikora, & Aberle, 2011). To assess changes in channel bed material, we used pebble-count data to calculate the percent change in the D_{50} , the grain size below which 50% of the bed material is finer. We tested for significant differences in grain size distributions during each time period using the Kolmogorov-Smirnov test. All statistical analyses were performed in R. In the unburned reference reach, MCR, which we only surveyed in June 2021, we repeated cross section and pebble count measurements taken by NEON staff in August 2019 and evaluated change between 2019 and 2021. This time span is similar to the study period in that it encompasses two winters in which flows at nearby gages were predominantly below the two-year recurrence interval flood. As such, we considered the change in MCR between 2019 and 2021 as representative of the magnitude of change that may have occurred during the study period.

To contextualize temporal changes in bed grain size and channel geometry in study reaches, we assessed flow competence (i.e., the ability of flow to mobilize bed material). This entailed calculation of boundary shear stress (τ_0) during the peak flow in WYs 2021 and 2022 and of the critical shear stress needed to mobilize the D_{50} . We determined peak-flow τ_0 values for each surveyed cross section from either HEC-RAS modeling (WRT, BOG, CON) or as:

$$\tau_0 = \rho g R S \quad (1)$$

where ρ is water density, g is acceleration due to gravity, R is hydraulic radius, and S is channel slope. We calculated the critical shear stress, τ_c , for mobilization of the D_{50} as:

$$\tau_c = \tau_c^* (\rho_s - \rho) g D_{50} \quad (2)$$

where ρ_s is sediment density and τ_c^* is dimensionless critical shear stress, calculated here using a slope-dependent equation developed for steep streams (Recking, 2009; Recking et al., 2012):

$$\tau_c^* = 0.15 S^{0.275} \quad (3)$$

Finally, we compared τ_0 (at peak flow) and τ_c to evaluate whether entrainment of the D_{50} is likely to have occurred (i.e., $\tau_0 > \tau_c$).

To provide insight on the influence of wildfire on instream large wood and associated effects on channel morphology, we assessed large wood conditions in burned reaches in March 2022 and in MCR in June 2021. To do so, we used a combination of ground photos and analysis of UAV imagery-derived, georeferenced orthophotos. We defined large wood to be any piece with a mid-length diameter ≥ 20 cm (the size that could be readily identified in orthophotos) that extended at least 1 m into the bankfull channel. We classified each piece as single or part of a jam (defined as three or more pieces of large wood in contact), and noted the presence or absence of a rootwad, features of accumulation, level of decay, burn status, stability, source, and whether the piece forced a geomorphic unit (e.g., pool, bar) and was storing sediment (Wohl et al., 2010).

4 | RESULTS

4.1 | Precipitation and hydrologic response

Total precipitation during the study period was below average in all sites, such that all Z-scores of total precipitation were negative (Table 2). The Z-scores were greater in WY 2022 and for sites in and near the Holiday Farm Fire (CON and MCR) than for Archie Creek Fire sites (Table 2). Consistent with typical regional hydroclimate patterns, most precipitation and streamflow occurred between October and April (Figure 3). Precipitation fell primarily as rain, with a greater proportion of snow in the higher-elevation MCR site. Study sites showed similar behaviour in terms of precipitation timing and intensity within Archie Creek or Holiday Farm sites, and variability between years (Table 2).

In some cases, daily precipitation maxima corresponded with peak flow (e.g., early January, 2022 in Archie Creek sites), but in other cases, there were lags between storms and runoff (e.g., for large, late-fall precipitation events). In general, stage hydrographs in burned reaches illustrate high-frequency, short-duration (i.e., less than two days) increases in stage in response to storm events. Stage increases in MCR were less frequent and longer duration, at least partly reflecting the greater prevalence of snow at this site. Precipitation maxima did not exceed published thresholds (Wiley, 2000) for landsliding, as discussed further below.

In the 1.5 years after the wildfires, peak flows in burned reaches remained mostly confined to the bankfull channel, according to pressure transducer measurements and hydraulic modeling. The peak discharges we estimated for these sites did not exceed 50% annual exceedance probability (i.e., 2-year recurrence interval) floods, which is consistent with nearby gaged sites.

TABLE 2 Precipitation data during study period.

		WRT	BOG	SWP	CON	MCR
Total ^a (mm)	WY 2021	1191	1134	1414	1786	1851
	WY 2022 ^b	811	752	987	1290	1333
% of normal ^{a,c}	WY 2021	74	75	71	84	83
	WY 2022 ^b	81	79	78	84	84
Z-score of log (total precipitation) ^{a,c,d}	WY 2021	-1.5	-1.4	-1.7	-0.83	-0.87
	WY 2022 ^b	-0.74	-0.84	-0.90	-0.60	-0.57
Max daily (mm) and date	WY 2021	37 ^e 11/18/20	37 ^e 11/18/20	37 ^e 11/18/20	65 ^f 12/20/20	65 ^f 12/20/20
	WY 2022 ^b	49 ^a 1/4/22	47 ^a 1/4/22	59 ^a 1/4/22	59 ^g 1/5/22	59 ^g 1/5/22
Max 24-h (mm) and date	WY 2021	58 ^e 11/15/20	58 ^e 11/15/20	58 ^e 11/15/20	80 ^f 12/20/20	80 ^f 12/20/20
	WY 2022 ^b	- -	- -	- -	67 ^g 1/5/22	67 ^g 1/5/22
Max 15-min intensity (mm h ⁻¹) and date	WY 2021	17 ^e 1/13/21	17 ^e 1/13/21	17 ^e 1/13/21	21 ^g 9/18/21	21 ^g 9/18/21
	WY 2022 ^{b,h}	- -	- -	- -	17 ^g 11/10/21	17 ^g 11/10/21

Abbreviations: WRT, Wright Creek; BOG, Bogus Creek; SWP, Swamp Creek; CON, Cone Creek; MCR, McRae Creek.

^aSource: PRISM Climate Group (2022).

^bFor the portion of WY 2022 encompassed by the study period (Oct. 2021 to Mar. 2022).

^cDerived from monthly average precipitation for 1991–2020.

^dBecause precipitation is log-normally distributed, we report Z-scores of the log-transformed total precipitation.

^eSource: Archie1 tipping bucket gage (1-min resolution, latitude 43.299731, longitude –122.801334, elevation 619 m).

^fSource: Holiday4 tipping bucket gage (1-min resolution, latitude 44.139128, longitude –122.334849, elevation 405 m).

^gSource: USGS Blue River Dam Met Station near Blue River, OR, #441016122194300.

^hNo data available for Archie Creek Fire sites in WY2022 at a resolution finer than daily.

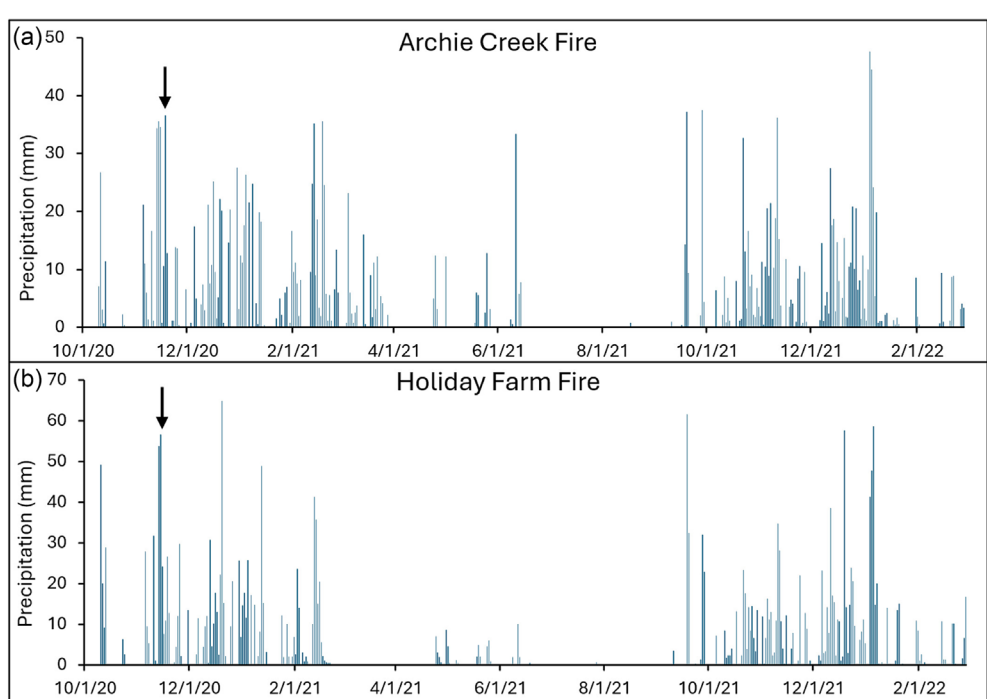


FIGURE 3 Daily precipitation during study period near (a) Archie Creek Fire (1 October 2020 to 4 November 2020 data from PRISM, 5 November 2020 to 16 September 2021 data from Archie1 tipping-bucket gage, 17 September 2021–28 February 2022 data from PRISM) and (b) Holiday Farm Fire study sites (1 October 2020 to 21 November 2020 data from USGS Cougar Dam Met Station Near Rainbow, OR, #440752122143200, 22 November 2020 to 10 September 2021 data from Holiday4 tipping-bucket gage, 11 September 2021 to 28 February 2022 data from USGS Blue River Dam Met Station near Blue River, OR, #441016122194300). Arrows denote mid-November 24-h, 58 mm (Archie Creek) and 76 mm (Holiday Farm) rain events prior to initial field surveys.

4.2 | Sediment, wood, and geomorphic response

Post-fire imagery from UAV surveys and trail cameras complemented ground surveys to document hillslope and channel responses at multiple spatial and temporal scales. The UAV surveys (Supplemental Video) did not show any evidence of post-fire mass wasting events in study watersheds, with the exception of two landslides in WRT basin, which we describe below. UAV surveys showed a high density of downed logs on the floor of burned hillslopes and adjacent valley bottoms, as well as illustrating the effects of variable burn severity, with some areas experiencing loss of all vegetation and organic litter on hillslopes, while other areas retaining intact trees.

Trail cameras showed changes in water colour suggestive of increased turbidity during high flows in burned study reaches but not in the unburned MCR reach during the first two winter–spring wet periods following the fire. Trail-camera observations were corroborated by turbidity measurements at a.

USGS gaging station on the North Umpqua River 18–25 km downstream of where the Archie Creek Fire study reaches enter the mainstem (USGS 14317450 North Umpqua River near Idleyd Park, OR), which showed short-duration turbidity spikes (hours to days), especially during the mid-November 2020 (prior to trail-camera installations) and early-January 2022 rainfall events (U.S. Geological Survey), 2024. Comparing timing of turbid flows to precipitation data suggests erosive overland flow occurred during storms exceeding a 24-hour, $\sim 1.6 \text{ mm h}^{-1}$ intensity. UAV surveys and field observations revealed little evidence of riling and gullying on burned slopes, suggesting that surface erosion occurred mainly as sheetwash.

Burned areas had abundant downed wood on hillslopes, in riparian areas, and in streams. We measured between 1.0 (BOG) and 1.8 (WRT) pieces of large wood per 10 m stream length in burned reaches (Figure 4); 85% of these pieces were partially or completely burned. We recorded slightly lower wood loading, 0.9 pieces per 10 m, in the unburned study reach, MCR, where all pieces showed signs of decay and did not appear to be recently recruited to the channel. About a third (29%) of large wood pieces formed channel-spanning jams in WRT, SWP, and CON; no jams were observed in BOG. Pieces that were not in jams were ramped at various angles in the channel, in some cases contributing to sediment aggradation and bar formation,

or were bridged across the channel in a manner that limited their hydraulic influence.

Study streams showed local, ephemeral adjustments in bed elevations, as shown by repeat longitudinal profile surveys (Figure 5), and in grain size (Figure 6), as discussed on a reach-by-reach basis below. Gross channel changes in width, depth, slope, and bed roughness height were limited (Table 3; Figures 5 and 6). Calculations of the boundary shear stresses at peak-flow conditions, compared to the critical shear stress required to mobilize bed materials, indicated that peak flows in burned reaches in WYs 2021 and 2022 were competent to transport the D_{50} at nearly all cross sections. In MCR, in contrast, flows were not competent to transport the D_{50} (Busby, 2022 provides details of flow competence calculations).

The most significant mass-wasting events were two landslides in the WRT basin, which occurred ~ 600 and 700 m upstream of the study reach as a result of road-fill failure during a 1-day, 49 mm rain event on 4 January 2022 (Figure 7; Table 2). The two landslides had volumes of $\sim 900 \text{ m}^3$ and $\sim 1200 \text{ m}^3$, as estimated from UAV imagery-derived DSMs in Pix4D, in some places scouring to bedrock, but differing degrees of connectivity to WRT. For the farther upstream landslide, which occurred in a tributary gully rated with high debris-flow hazard (U.S. Geological Survey), 2020, we estimated a sediment delivery ratio (SDR, i.e., the ratio of sediment delivered to the stream to the total volume of sediment in the landslide) of 83% (i.e., $\sim 750 \text{ m}^3$ of sediment entered WRT). The landslide produced a debris fan comprised mostly of fine sediment and large wood (Figure 7(c)) that forced a channel constriction and local gradient adjustments, with a pool on the upstream side, and a transient knickpoint on the downstream side. The downstream of the two landslides had an SDR of 25% (i.e., $\sim 300 \text{ m}^3$ of sediment entered WRT) and deposited a debris fan of mostly cobble and boulder-sized sediment and some large wood adjacent to the creek (Figure 7(e)). Trail cameras showed changes in the colour of streamflow in WRT following the landslides, suggestive of turbidity increases, lasting for two days. Turbidity increases were also recorded at the USGS North Umpqua River near Idleyd Park, OR gaging station, 25 km downstream of where WRT enters, during the early January 2022 rainfall event, from background levels of 2–3 FNU (formazin nephelometric units) to a peak of 112 NTU (U.S. Geological Survey), 2024.

In WRT, during the second winter rainy season after the fires, there was significant bed-material coarsening, and the D_{50} increased by 52% (Table 3; Figure 6). Although changes in average bankfull depth were not significant (Table 3), repeat longitudinal profiles show $\sim 0.7 \text{ m}$ of incision in the upper portion of the reach between December 2020 and March 2022 (Figure 5).

BOG showed the most immediate geomorphic response to the fires. As of initial field surveys, 1.5 months after the fires, we observed a small landslide/slump along the channel margin (Figure 6), a rill and associated fan of fine to cobble-sized sediment on the floodplain just upstream of the study reach, and fresh overbank fine-sediment deposition and gravel aggradation within the channel. Based on their appearance and mobility, we infer that these erosional and depositional features are post-fire (Figures 6, 8, 9), most likely as a result of the mid-November 2021 precipitation event described above. Gravel aggradation in BOG mostly persisted during the first winter after the fires, and further aggradation occurred locally, but this sediment was largely eroded during the second winter rainy season (Figures 5, 9).

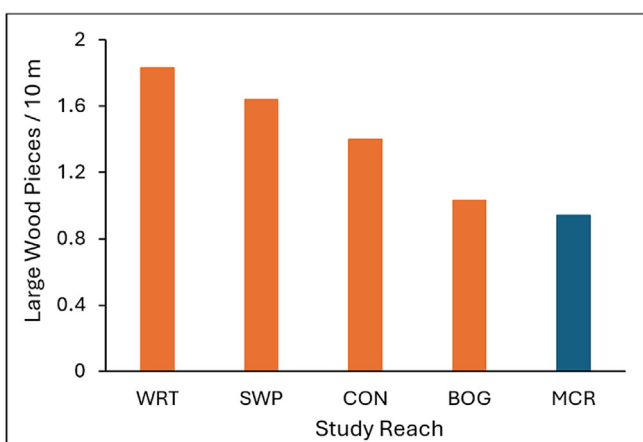


FIGURE 4 Large wood pieces per 10 m stream length in burned (orange) and unburned (blue) study reaches.

FIGURE 5 Thalweg longitudinal profiles of study reaches, showing localized aggradation and incision. Vertical changes were mostly less than 0.3 m, with the exception of ~0.7 m of degradation in WRT (A) at distance 15 m between December 2020 and March 2022. Because the thalweg location sometimes shifted between surveys, plots do not depict repeat surveys of identical locations. Note differing vertical exaggeration on each plot.

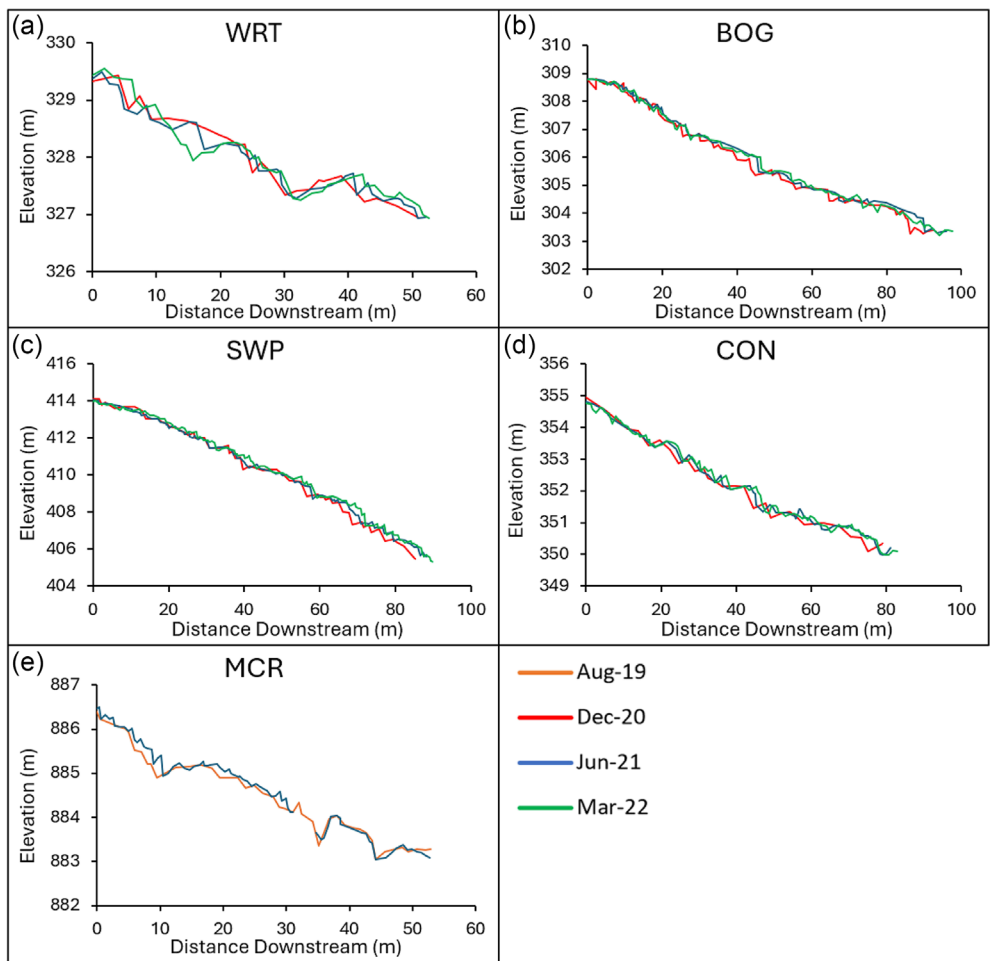


FIGURE 6 Grain size distributions in study reaches. There were statistically significant changes in grain size between December 2020 and June 2021 in (c) SWP and (d) CON, between June 2021 and March 2022 in (a) WRT, and between December 2020 and March 2022 in (b) BOG, (c) SWP, and (d) CON. Gray dashed line indicates D_{50} . CON, Cone Creek; SWP, Swamp Creek; WRT, Wright Creek.

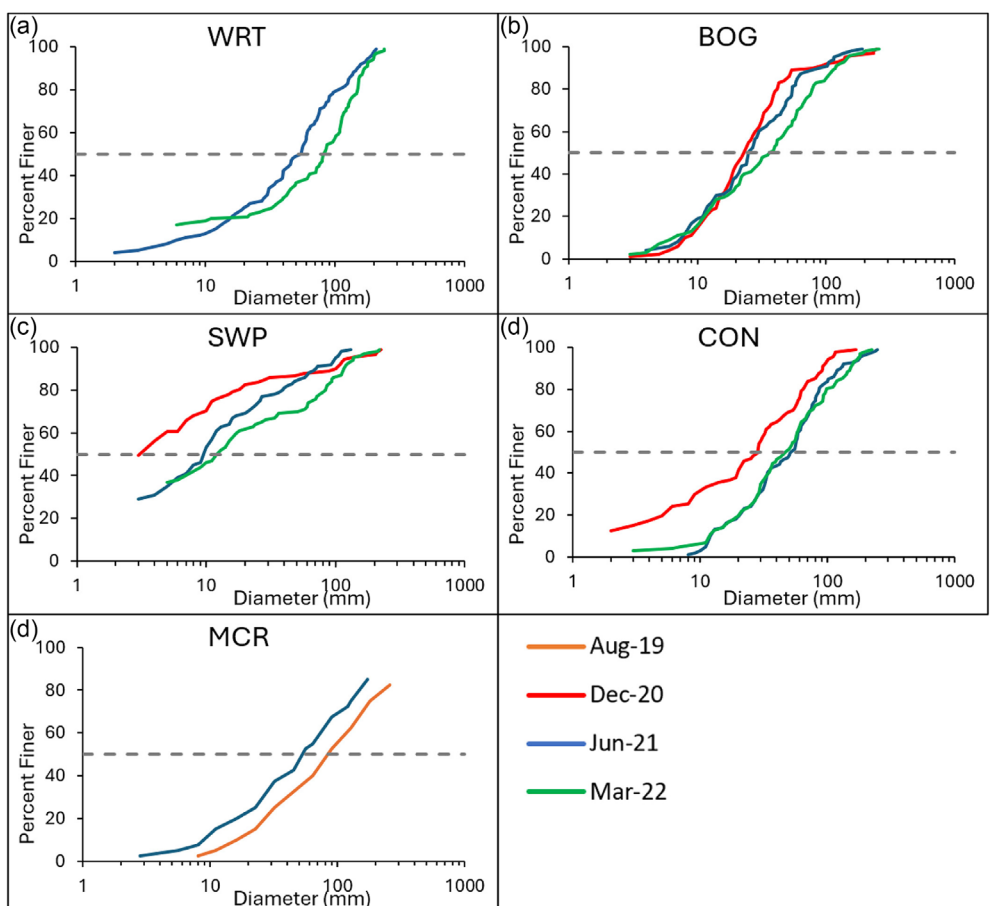


TABLE 3 Summary of channel morphology measurements in study reaches: average bankfull depth (h_{bf}) and width (w_{bf}), median grain size (D_{50}), bed slope (S_o), and bed roughness height^a.

Site	Survey date	h_{bf} ^b (m)	w_{bf} ^b (m)	D_{50} ^b (mm)	S_o	Bed roughness height
WRT	Dec-20	0.94	7.7	–	0.048	0.20 m
	Jun-21	0.68	6.9	54	0.043	0.20 m
	Mar-22	0.77	8.2	82*	0.043	0.26 m
BOG	Dec-20	0.59	5.9	23	0.060	0.26 m
	Jun-21	0.60	6.1	24	0.060	0.25 m
	Mar-22	0.61	5.3	36**	0.059	0.21 m
SWP	Dec-20	0.48	2.4	3	0.100	0.28 m
	Jun-21	0.51	2.4	10*	0.097	0.23 m
	Mar-22	0.64	2.4	12**	0.097	0.29 m
CON	Dec-20	0.52	9.0	28	0.059	0.24 m
	Jun-21	0.57	9.0	52*	0.056	0.21 m
	Mar-22	0.76	9.2	47**	0.057	0.19 m
MCR ^b	Aug-19	0.34	4.7	90		
	Jun-21	0.36	4.5	56		

Abbreviations: WRT, Wright Creek; BOG, Bogus Creek; SWP, Swamp Creek; CON, Cone Creek; MCR, McRae Creek.

^aBed roughness height is calculated as the standard deviation of the thalweg elevation, from longitudinal profiles.

^bNone of the changes in bankfull depth or width were statistically significant ($P < 0.05$). Statistical testing was not performed for depth and width changes on MCR.

*Statistically significant difference ($P < 0.05$), between December 2020 and June 2021. **Statistically significant difference ($P < 0.05$), between December 2020 and March 2022 (i.e., over the length of the study period).

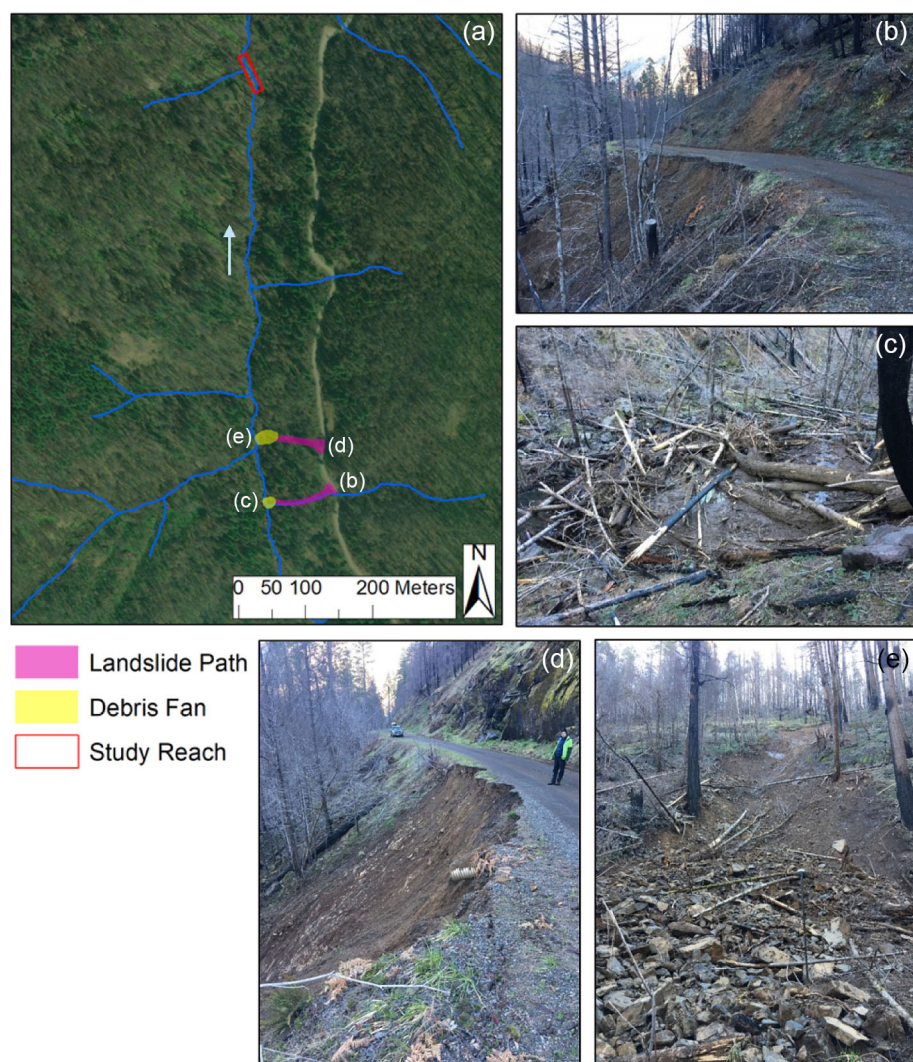


FIGURE 7 Landslides in WRT basin, which burned in the Archie Creek Fire, triggered from road-fill failure in January 2022. (a) Landslide, stream, and study reach locations. Blue arrow indicates flow direction, and letters denote locations of ground photos in panels b–e: upstream and downstream landslide initiation sites (b and d, respectively), upstream debris fan of mostly fine sediment and large wood (c), and downstream debris fan of cobble to boulder-sized sediment and large wood (e). WRT, Wright Creek.

This is consistent with repeat pebble counts, which showed only a 4% change in the D_{50} during the first winter and a 50% increase during the second winter (Table 3; Figure 6), reflecting bed-material coarsening. Only the change in grain size distribution between December 2020 and March 2022 (57% increase in D_{50}) was statistically significant (Table 3; Figure 6).

SWP, the steepest and smallest-drainage area study reach, exhibited the most continuous step-pool system, with boulder and wood steps, an entrenched channel, and undercut banks (Figure 10). The D_{50} (excluding step-forming boulders) was 3 mm 1.5 months after the fires (Table 3), suggesting substantial fine-sediment supply and fine-sediment trapping by steps and in pools. Subsequent surveys showed incision (32% increase; +0.16 m in average bankfull depth during the study, but not statistically significant) and significant bed-material coarsening over the study period (300% increase in D_{50} ; Table 3; Figure 6).



FIGURE 8 BOG study reach in December 2020, showing post-fire geomorphic change (inferred from observational evidence) including treefall, slumping, and a mid-channel gravel bar; blue arrow indicates flow direction. BOG, Bogus Creek.

Channel conditions in CON fluctuated following the fires. Initial surveys documented what appeared to be new, post-fire marginal channel bar deposition comprising fine to cobble-sized sediment at the downstream end of CON, as well as overbank fine-sediment deposition. During the first winter rainy season after the fires, the marginal bar began to erode, and a mid-channel bar formed (by June 2021) and then eroded (by March 2022) (Figure 11). As of March 2022, bank erosion resulted in localized widening and deepening of the bankfull channel (Figure 11(c)), although reach-averaged changes were not statistically significant (Table 3). Ground photos showed substantial gravel deposition above wood jams at the upstream and downstream ends of the reach during the initial rainy season, which persisted through the second rainy season. Bed material coarsened significantly (86% increase in D_{50}) during the initial winter, and then remained consistent (Table 3; Figure 6). Two channel-margin slumps occurred at the downstream end of CON during the second winter



FIGURE 10 SWP study reach in December 2020, showing steep, entrenched, step-pool channel. SWP, Swamp Creek.

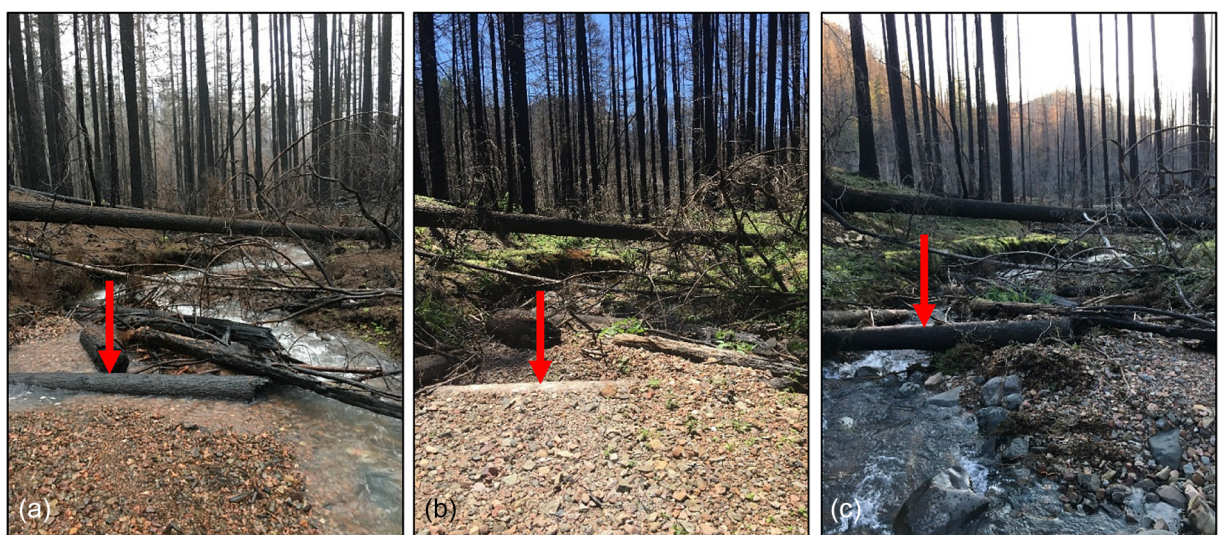


FIGURE 9 Repeat photos looking downstream in BOG study reach showing wood-forced gravel aggradation between (a) December 2020 and (b) June 2021 and erosion by (c) March 2022. Between (b) and (c), there was >0.6 m of channel incision at the location indicated by the arrow. BOG, Bogus Creek.



FIGURE 11 Repeat photos looking upstream in CON showing mid-channel bar formation between (a) December 2020 and (b) June 2021 and erosion by (c) March 2022, as well as bank erosion and channel widening in (c). CON, Cone Creek.

rainy season after the fires, creating additional sediment supply and geomorphic change.

MCR appeared to be morphologically stable from August 2019 to June 2021. Thalweg (Figure 5) and cross-section surveys showed consistent channel morphology, and time-lapse photos showed no noticeable changes in channel morphology at the trail camera location during this period. Although the D_{50} decreased by 38%, the change in grain size distribution was not significant (Table 3; Figure 6).

5 | DISCUSSION

Our observations shed light on the influence of tiered controls on the hydrogeomorphic responses to wildfire (Figure 1). The high burn severity of the 2020 fires, steep topography, and high long-term mean annual precipitation of study basins (Table 1) suggested that these streams would be susceptible to geomorphic change from post-fire flooding and debris flows. On the one hand, the post-fire sediment-supply increases, wood recruitment, and resultant sequence of channel aggradation followed by erosion in burned reaches that we observed are consistent with previous studies of steep stream response to wildfire (e.g. Florsheim et al., 2017; Florsheim & Chin, 2024; Florsheim, Keller, & Best, 1991; Keller, Valentine, & Gibbs, 1997; Minshall, Robinson, & Lawrence, 1997). On the other

hand, our streams did not show substantial morphologic change during the study period, owing to the absence of debris flows or floods large enough to mobilize the coarser fractions of bed material, which we elaborate on below.

The muted hydrogeomorphic response we observed in burned reaches highlights the importance of post-fire precipitation, including below-average precipitation, as occurred in the study period (e.g. Brogan, Nelson, & MacDonald, 2019; Chin et al., 2019). In the future, precipitation that exceeds thresholds for flooding and debris flows could trigger destabilization in study sites, particularly within the time period of maximum vulnerability when pre-fire vegetation roots have decayed and post-fire regrowth is limited, ideas that we explore further below. Alternatively, steep streams may prove resilient to destabilization even during large floods, and high transport capacities may be sufficient to flush large inputs of sediment without reorganization of channel-bed structure, especially if those sediment inputs are finer than the antecedent bed material. The high infiltration capacity of soils in the region, where infiltration-excess overland flow is rare even after wildfire (Wondzell & King, 2003), as well as the highly localized nature of fire effects on soil hydrological properties (McGuire et al., 2018), also would tend to dampen fire-induced increases in runoff in the study area. Erosive overland flow only occurred in the study basins, as suggested by qualitative trail camera evidence of turbidity increases, during a few storms exceeding a

24-hour, $\sim 1.6 \text{ mm h}^{-1}$ intensity. These observations, coupled with the near-absence of landslides, suggest that post-fire erosion in the burned watersheds we monitored occurred primarily as surface erosion.

Streams did show some changes in the post-fire period, indicative of transient, dynamic conditions as a result of shifts in the balance of sediment supply and transport capacity. Burned reaches exhibited changes in bed-material size and local changes in channel geometry from aggradation and erosion, although changes in gross channel form (e.g., average bankfull width and depth, slope) were limited. Burned sites appeared to be in sediment transport-limited conditions in the first winter rainy season after the fires (i.e., sediment supply was high relative to transport capacity), as a result of post-fire increases in sediment supply and wood recruitment, contrary to the typical supply-limited conditions in steep streams. After the wildfires, the amount of large wood pieces in burned reaches increased by $\sim 50\%$, increasing flow resistance and reducing transport capacity. The coarse sediment aggradation we observed during the first post-fire winter in BOG and CON, which reduced wetted channel area, is suggestive of high sediment supply in these sites, which may reflect the combination of steep basin slopes and high burn severity in the BOG and CON basins (Table 1). In addition, accumulation of gravel to finer-sized sediment in channels decreased bed grain size and in turn lowered bed-mobility thresholds, facilitating evacuation of new sediment deposits even at modest flows.

During the second winter after the fires, streams evolved toward supply-limited conditions. Peak flows exceeded critical shear stress for mobilization of the D_{50} , leading to flushing of fine sediments, significant coarsening of channel bed material, and incision of post-wildfire sediment deposits, suggesting a trajectory of recovery to pre-fire bed-material conditions. In SWP, for example, our observations suggest that, despite evidence of local sediment supply increases from bank collapse and erosion around a rootwad, there was flushing of fine sediments over the study period that resulted in channel degradation. The pattern of evolution toward supply limitation applies even in WRT, where two landslides in January 2022 increased sediment supply. There was an inferred spike in turbidity in WRT following the landslides, based on trail-camera images, but we posit that coarser sediment delivered to the channel had not yet been transported to our reach during the study period, perhaps due to reduced transport capacity associated with post-fire wood loading, and suggesting different time scales of fine versus coarse sediment routing through the channel network.

Transient increases in turbidity and sediment accumulation in study reaches may be deleterious to aquatic habitat (Wood & Armitage, 1997) and represent a short-term threat to spawning success for salmonids and lamprey (Federal Emergency Management Agency (FEMA), 2020). Further, channel aggradation can cause summer base flows to drop below the level of the bed, creating discontinuities in the wetted channel and reducing pool capacity (May & Lee, 2004). We anticipate that, in the absence of debris flows, post-fire recruitment of large wood will likely have the most prolonged effect on biophysical processes in the study streams by creating habitat complexity (e.g. Fausch & Northcote, 1992) and roughness, reducing transport capacity, and mediating downstream sediment delivery (Chin et al., 2024; Montgomery et al., 2003; Welling, Wilcox, & Dixon, 2021; Wohl et al., 2022).

Spatial and temporal variability in climate and other controls identified in Table 1 may manifest as different types of erosional responses (e.g., surface erosion versus mass wasting) across watersheds, occurring at different times since a disturbance. In the time since we completed field work, mass-wasting events have occurred in the Archie Creek and Holiday Farm burn areas, although we are not aware of any that directly affected study reaches. For example, a road-induced landslide occurred in the SWP basin, downstream of our study reach, in spring 2022. Multiple landslides or debris flows occurred in the Archie Creek burn area on 13 January 2024; 28.5–46 mm of rain was recorded that day at nearby gages (Roseburg, OR and Toketee Falls, OR).

Post-fire landscape changes may also be influenced by management activities implemented in response to fire, including salvage logging and hazard-tree removal operations. These activities are common following wildfire, including in the study area, and they remove large wood from the landscape that stores sediment on hillslopes (Adams et al., 2023) and in channels (Welling et al., 2021; Rengers et al., 2023). Post-fire salvage logging may also increase hillslope runoff and erosion rates, although increases depend strongly on watershed characteristics and logging methods (McIver & Starr, 2001).

Our analysis illustrates complexities of considering geomorphic change in terms of exceedance of thresholds, the identification and analysis of which is fundamental in geomorphology (Church, 2002). On the one hand, shear-stress thresholds for mobilizing the median grain size of bed material (excluding boulders) were exceeded, such that localized sediment transport, aggradation, and erosion occurred. On the other hand, substantial channel reorganization did not occur, and larger clasts remained immobile. In steep streams with step-pool morphology, size fractions coarser than the median are typically mobile only during large floods (Gilbert & Wilcox, 2024; Mao et al., 2008), and step-forming boulders serve as keystones for controlling channel morphology (Chin, 1989; Church & Zimmermann, 2007).

Moreover, thresholds to trigger debris flows were not exceeded during the study period. Debris-flow triggering precipitation thresholds (e.g. Jakob & Hungr, 2005; Pitlick, 1994) are typically estimated using either statistical or empirical methods (e.g. Staley et al., 2017). For western Oregon, Wiley (2000) suggests the following threshold conditions for all “fast-moving landslides,” inclusive of debris flows: (1) $\sim 20 \text{ cm}$ of antecedent rain since the end of September, which typically marks the onset of the rainy season, based on the concept that wet antecedent soils facilitate instability, and (2) 24-h rainfall exceeding 40% of mean December rainfall. Wiley’s (2000) threshold does not explicitly consider wildfire, roads, and timber harvest history. In our study area, Wiley’s (2000) antecedent rainfall requirement was exceeded in early to mid-November in all sites and in both years, but the 24-hour precipitation thresholds (40% of mean December rainfall equates to 113–147 mm, depending on the site) were not exceeded (Table 2). The two road-fill failure landslides in WRT occurred in response to an unexceptional storm (49 mm rainfall event on 4 January 2022; Figure 7), which is well below Wiley’s suggested threshold, illustrating the potential for wildfire and road development to lower precipitation thresholds for landslides.

We also evaluated precipitation data relative to USGS statistical models of debris-flow likelihood, which classified three of the burned study streams as having high debris-flow hazard in response to a

15-min, 24 mm h⁻¹ rain event (U.S. Geological Survey, 2020). This threshold was not exceeded during the study period (Table 2). More generally, there is a critical need for refinement of rainfall thresholds for triggering post-fire debris flows in western Oregon (Thomas et al., 2023), especially in light of projected increases in fire frequency and severity across the Pacific Northwest under climate change (e.g. Halofsky, Peterson, & Harvey, 2020; Littell et al., 2018).

Rainfall intensity-duration thresholds change following wildfire as soil infiltration capacity, canopy cover, root strength, and hydraulic roughness of the ground surface evolve, in a manner that varies based on both site-specific and hydroclimatic factors (Hoch et al., 2021; Raymond et al., 2020). Post-fire landscape responses may be most likely during a “window of disturbance” timescale (Hoch et al., 2021); linkage of mechanistic models of vegetation regrowth with physically based, distributed hydrologic models is a key need in terms of modeling how post-fire systems recover (Ebel et al., 2023). Hillslope susceptibility to erosion may be prolonged by drought in the years following wildfire, which may slow vegetation recovery, delay or prevent reestablishment of root systems and associated stabilization of hillslopes (Hatchett et al., 2021), and/or result in the conversion of pre-fire forest to nonforest vegetation (Coop et al., 2020).

Much of the western United States experienced extended drought in the first two decades of the 21st century (Williams, Cook, & Smerdon, 2022). Severe drought conditions also characterized Oregon’s climate during that period, including in the study area in the months preceding the 2020 fires (O’Neill, Hatchett, & Dalton, 2021), and drought continued during the study period. Both the extended drought and increased fuel aridity, which created conditions ripe for the 2020 wildfires in the Western Cascades (Abatzoglou et al., 2021), have been attributed to human-induced climate change (Abatzoglou & Williams, 2016; Williams, Cook, & Smerdon, 2022). The muted post-fire responses in study streams, reflecting below-average precipitation during the post-fire period, may also bear the direct or indirect signature of climate change, which could also affect the window-of-disturbance timescale (McGuire et al., 2019) and forest-regeneration patterns (Davis et al., 2019) in a manner that alters hillslope hydrology and sediment dynamics. Conversely, intense precipitation events in western Oregon are projected to increase in frequency in response to climate change (Cooley & Chang, 2021; Touma et al., 2022), which would heighten potential for post-fire flooding and debris flows. Climate change may thus have complex, multifaceted effects on post-fire landscape response.

6 | CONCLUSION

Changes in fluxes of water, sediment, and large wood after severe wildfire in the Western Cascades induced an evolving balance of sediment supply to transport capacity in steep streams affected by the 2020 Labor Day fires. Bed-material size exhibited the greatest change among the geomorphic parameters we measured, while gross channel form showed resilience, despite local aggradation and erosion. Post-fire inputs of large wood will likely have prolonged implications for channel morphology and habitat heterogeneity. Landscape responses to disturbance may not manifest for years to decades, as a function of precipitation, vegetation change, management actions, and short-term sediment disconnectivity that creates time lags between hillslope and

fluvial responses (e.g. Fryirs, 2013). Climate change may exert a complex influence on channel response to wildfire by increasing drought (i.e., lowering total precipitation) while simultaneously increasing the frequency of extreme rain events and the duration of susceptibility to disturbance.

AUTHOR CONTRIBUTIONS

David Busby: Conceptualization; funding acquisition; methodology; investigation; resources; writing—initial draft. **Andrew Wilcox:** Conceptualization; funding acquisition; methodology; investigation; supervision; writing—reviewing and editing.

ACKNOWLEDGEMENTS

This work was supported by the National Science Foundation [DGE 1633831, EAR1644619], the North Umpqua Foundation, and a Geological Society of America Graduate Research Grant. We thank Claire Gilder, Jordan Gilbert, Marco Maneta, Phil Higuera, Vince Archer, and Andy Efta for research guidance; Nicole Cleland and Wendell Elliott for field assistance; Ben Vierra, Chris Burton, and Nick Harrison for supporting NEON data collection; Kevan Moffett, Mark Sommer, and Cheryl Friesen for assistance with field access and permissions; Josh Roering for trail cameras and precipitation data sharing; Mike Grilliot for conducting drone surveys; Jaylene Naylor for assistance with drone survey logistics; and Rich Grost, Becky McRae, and Ed Kikimoto for other ground/field support. We also thank the reviewers for suggestions that greatly improved the manuscript.

CONFLICT OF INTEREST STATEMENT

The authors declare no conflicts of interest.

DATA AVAILABILITY STATEMENT

Data supporting this study are presented in their entirety in Busby (2022).

ORCID

Andrew C. Wilcox  <https://orcid.org/0000-0002-6241-8977>

REFERENCES

Abatzoglou, J.T., Rupp, D.E., O’Neill, L.W. & Sadegh, M. (2021) Compound extremes drive the western Oregon wildfires of September 2020. *Geophysical Research Letters*, 48(8), 1–9. Available from: <https://doi.org/10.1029/2021GL092520>

Abatzoglou, J.T. & Williams, A.P. (2016) Impact of anthropogenic climate change on wildfire across western US forests. *Proceedings of the National Academy of Sciences of the United States of America*, 113(42), 11770–11775. Available from: <https://doi.org/10.1073/pnas.1607171113>

Adams, K. V., Dixon, J. L., Wilcox, A. C. & McWethy, D. (2023). Fire-produced coarse woody debris and its role in sediment storage on hillslopes. *Earth Surface Processes and Landforms*, 48, 1665–1678. <https://doi.org/10.1002/esp.5573>

Benda, L. (1990) The influence of debris flows on channels and valley floors in the Oregon coast range, U.S.a. *Earth Surface Processes and Landforms*, 15(5), 457–466. Available from: <https://doi.org/10.1002/esp.3290150508>

Benda, L. & Dunne, T. (1997) Stochastic forcing of sediment supply to channel networks from landsliding and debris flow. *Water Resources Research*, 33(12), 2849–2863. Available from: <https://doi.org/10.1029/97WR02388>

Benda, L., Miller, D., Bigelow, P. & Andras, K. (2003) Effects of post-wildfire erosion on channel environments, Boise River, Idaho. *Forest*

Ecology and Management, 178(1-2), 105–119. Available from: [https://doi.org/10.1016/S0378-1127\(03\)00056-2](https://doi.org/10.1016/S0378-1127(03)00056-2)

Benda, L., Veldhuisen, C. & Black, J. (2003) Debris flows as agents of morphological heterogeneity at low-order confluences, Olympic Mountains, Washington. *Geological Society of America Bulletin*, 115(9), 1110–1121. Available from: <https://doi.org/10.1130/B25265.1>

Bigelow, P.E., Benda, L.E., Miller, D.J. & Burnett, K.M. (2007) On debris flows, river networks, and the spatial structure of channel morphology. *Forest Science*, 53(2), 220–238. Available from: <https://doi.org/10.1093/forestscience/53.2.220>

Brogan, D.J., Nelson, P.A. & MacDonald, L.H. (2019) Spatial and temporal patterns of sediment storage and erosion following a wildfire and extreme flood. *Earth Surface Dynamics*, 7(2), 563–590. Available from: <https://doi.org/10.5194/esurf-7-563-2019>

Busby, D.M. (2022) *Hydrogeomorphic response of steep streams following severe wildfire in the Western Cascades, Oregon*. (Thesis). Department of Geosciences, University of Montana, Missoula, MT. <https://scholarworks.umt.edu/etd/11995/>

Calhoun, N., Burns, W., Kean, J. & Rengers, F. (2022) Recent observations of post-fire debris flows in five megafires in the Western Cascades, Oregon, Geological Society of America Annual Meeting, Denver, CO. Abstract 141–110.

Cerdá, A. & Doerr, S.H. (2005) Influence of vegetation recovery on soil hydrology and erodibility following fire: an 11-year investigation. *International Journal of Wildland Fire*, 14(4), 423–437. Available from: <https://doi.org/10.1071/WF05044>

Chin, A. (1989) Step pools in stream channels. *Progress in Physical Geography*, 13, 390–407.

Chin, A., Burton, J.W., Humphreys, K.M., Florsheim, J.L., Kinoshita, A.M., Andreano, E.C., et al. (2024) Vegetation and channel recovery ten years following the Waldo Canyon Fire of Colorado. In: Florsheim, J.-L., O'Dowd, A.P. & Chin, A. (Eds.) *Biogeomorphic responses to wildfire in fluvial ecosystems* (pp. 27–42). Geological Society of America, Special Paper 562. [https://doi.org/10.1130/2024.2562\(02\)](https://doi.org/10.1130/2024.2562(02))

Chin, A., Solverson, A.P., O'Dowd, A.P., Florsheim, J.L., Kinoshita, A.M., Nourbakhshbeidokhti, S., et al. (2019) Interacting geomorphic and ecological response of step-pool streams after wildfire. *Geological Society of America Bulletin*, 131(9–10), 1480–1500. Available from: <https://doi.org/10.1130/B35049.1>

Church, M. (2002) Geomorphic thresholds in riverine landscapes. *Freshwater Biology*, 47(4), 541–557. Available from: <https://doi.org/10.1046/j.1365-2427.2002.00919.x>

Church, M. (2006) Bed material transport and the morphology of alluvial river channels. *Annual Review of Earth and Planetary Science*, 34(1), 325–356. Available from: <https://doi.org/10.1146/annurev.earth.33.092203.122721>

Church, M. & Zimmerman, A. (2007) Form and stability of step-pool channels: research progress. *Water Resources Research*, 43(3), W03415. Available from: <https://doi.org/10.1029/2006WR005037>

Coble, A.A., Penaluna, B.E., Six, L.J. & Verschueren, J. (2023) Fire severity influences large wood and stream ecosystem responses in western Oregon watersheds. *Fire Ecology*, 19(1), 34. Available from: <https://doi.org/10.1186/s42408-023-00192-5>

Coleman, S.E., Nikora, V.I. & Aberle, J. (2011) Interpretation of alluvial beds through bed-elevation distribution moments. *Water Resources Research*, 47(11), 1–14. Available from: <https://doi.org/10.1029/2011WR010672>

Comiti, F. & Mao, L. (2012) Recent advances in the dynamics of steep channels. In: Church, M., Biron, P. M. & Roy, A. G. (Eds.), *Gravel-Bed Rivers: Processes, Tools, Environments*, 351–377. Wiley-Blackwell, NJ, United States. Available from: <https://doi.org/10.1002/9781119952497.ch26>

Conrey, R.M., Sherrod, D.R., Donnelly-Nolan, J.M. & Taylor, E.M. (2002) The North-Central Oregon Cascade margin: exploring petrologic and tectonic intimacy in a propagating intra-arc rift, in field guide to geologic processes in Cascadia. *Oregon Department of Geology and Mineral Industries Special Paper*, 26, 47–90.

Cooley, A.K. & Chang, H. (2021) Detecting change in precipitation indices using observed (1977–2016) and modeled future climate data in Portland, Oregon, USA. *Journal of Water and Climate Change*, 12(4), 1135–1153. Available from: <https://doi.org/10.2166/wcc.2020.043>

Coop, J.D., Parks, S.A., Stevens-Rumann, C.S., Crausbay, S.D., Higuera, P.E., Hurteau, M.D., et al. (2020) Wildfire-driven forest conversion in western North American landscapes. *Bioscience*, 70(8), 659–673. Available from: <https://doi.org/10.1093/biosci/biaa061>

Davis, K.T., Dobrowski, S.Z., Higuera, P.E., Holden, Z.A., Veblen, T.T., Rother, M.T., et al. (2019) Wildfires and climate change push low-elevation forests across a critical climate threshold for tree regeneration. *National Academy of Sciences of the United States of America*, 116(13), 6193–6198. Available from: <https://doi.org/10.1073/pnas.1815107116>

Ebel, B.A., Shephard, Z.M., Walvoord, M.A., Murphy, S.F., Partridge, T.F. & Perkins, K.S. (2023) Modeling post-wildfire hydrologic response: review and future directions for applications of physically based distributed simulation. *Earth's Futures*, 11(2), e2022EF003038. Available from: <https://doi.org/10.1029/2022EF003038>

Fausch, K.D. & Northcote, T.G. (1992) Large woody debris and salmonid habitat in a small coastal British Columbia stream. *Canadian Journal of Fisheries and Aquatic Sciences*, 49(4), 682–693. Available from: <https://doi.org/10.1139/f92-077>

Federal Emergency Management Agency (FEMA). (2020) Archie Creek Fire Erosion Threat Assessment/Reduction Team (ETART) summary report, December, <https://gscdn.govshare.site/1aa8ace4addf06592a8d7dc775413bf10fd1ec6/ETARTSummary-ArchieFire.pdf>

Florsheim, J.L. & Chin, A. (2024) Disturbance and recovery of physical elements of habitat in relation to post-wildfire channel sedimentation, southern California Transverse Ranges. In: Florsheim, J.L., O'Dowd, A.P. & Chin, A. (Eds.) *Biogeomorphic responses to wildfire in fluvial ecosystems*. Geological Society of America Special Paper, Colorado, United States. [https://doi.org/10.1130/2024.2562\(04\)](https://doi.org/10.1130/2024.2562(04))

Florsheim, J.L., Chin, A., Kinoshita, A.M. & Nourbakhshbeidokhti, S. (2017) Effect of storms during drought on post-wildfire recovery of channel sediment dynamics and habitat in the southern California chaparral, USA. *Earth Surface Processes and Landforms*, 42(10), 1482–1492. Available from: <https://doi.org/10.1002/esp.4117>

Florsheim, J.L., Keller, E.A. & Best, D.W. (1991) Fluvial sediment transport in response to moderate storm flows following chaparral wildfire, Ventura County, southern California. *Geological Society of America Bulletin*, 103(4), 504–511. Available from: [https://doi.org/10.1130/0016-7606\(1991\)103<0504:FSTIRT>2.3.CO;2](https://doi.org/10.1130/0016-7606(1991)103<0504:FSTIRT>2.3.CO;2)

Florsheim, J.L., O'Dowd, A.P. & Chin, A. (2024) *Biogeomorphic responses to wildfire in fluvial ecosystems*. Geological Society of America Special Paper, Colorado, United States 562, Available from: <https://doi.org/10.1130/SPE562>

Fryirs, K. (2013) (dis) connectivity in catchment sediment cascades: a fresh look at the sediment delivery problem. *Earth Surface Processes and Landforms*, 38(1), 30–46. Available from: <https://doi.org/10.1002/esp.3242>

Germanoski, D. & Miller, J.R. (1995) Geomorphic response to wildfire in an arid watershed, crow canyon, Nevada. *Physical Geography*, 16(3), 243–256. Available from: <https://doi.org/10.1080/02723646.1995.10642552>

Gilbert, J. & Wilcox, A.C. (2024) Estimating grain stress and distinguishing between mobility and transportability improves bedload transport estimates in coarse-bedded mountain rivers. *Journal of Geophysical Research-Earth Surface*, 129(8), e2024JF007662. Available from: <https://doi.org/10.1029/2024JF007662>

Grant, G.E., Swanson, F.J. & Wolman, M.G. (1990) Pattern and origin of stepped-bed morphology in high-gradient streams, Western cascades, Oregon. *Geological Society of America Bulletin*, 102(3), 340–352. Available from: [https://doi.org/10.1130/0016-7606\(1990\)102<0340:PAOOSB>2.3.CO;2](https://doi.org/10.1130/0016-7606(1990)102<0340:PAOOSB>2.3.CO;2)

Halofsky, J.E., Peterson, D.L. & Harvey, B.J. (2020) Changing wildfire, changing forests: the effects of climate change on fire regimes and vegetation in the Pacific northwest, USA. *Fire Ecology*, 16(1), 4. Available from: <https://doi.org/10.1186/s42408-019-0062-8>

Hatchett, B., McGuire, L., Youberg, A., Hoch, O., Oakley, N., McEvoy, D., Albano, C. & Lancaster, J. (2021) The role of drought in the

persistence of post-fire hydrologic hazards. Abstract H53G-06, AGU Fall Meeting, New Orleans, LA, 13-17 December.

Haugo, R.D., Kellogg, B.S., Cansler, C.A., Kolden, C.A., Kemp, K.B., Robertson, J.C., et al. (2019) The missing fire: quantifying human exclusion of wildfire in Pacific northwest forests, USA. *Ecosphere*, 10(4), e02702. Available from: <https://doi.org/10.1002/ecs2.2702>

Hoch, O.J., McGuire, L.A., Youberg, A.M. & Rengers, F.K. (2021) Hydrogeomorphic recovery and temporal changes in rainfall thresholds for debris flows following wildfire. *Journal of Geophysical Research: Earth Surface*, 126(12), e2021JF006374. Available from: <https://doi.org/10.1029/2021JF006374>

Hoffman, D.F. & Gabet, E.J. (2007) Effects of sediment pulses on channel morphology in a gravel-bed river. *Geological Society of America Bulletin*, 119(1-2), 116-125. Available from: <https://doi.org/10.1130/B25982.1>

Hyde, K., Jencso, K., Wilcox, A.C. & Woods, S. (2016) The influence of vegetation disturbance on hydrogeomorphic response following wildfire. *Hydrological Processes*, 30(7), 1131-1148. Available from: <https://doi.org/10.1002/hyp.10691>

Jackson, M. & Roering, J.J. (2009) Post-fire geomorphic response in steep, forested landscapes: Oregon coast range, USA. *Quaternary Science Reviews*, 28(11-12), 1131-1146. Available from: <https://doi.org/10.1016/j.quascirev.2008.05.003>

Jakob, M. & Hungr, O. (2005) *Debris-flow hazards and related phenomena*. Berlin, Germany: Springer 739 p.

Jefferson, A., Grant, G.E., Lewis, S.L. & Lancaster, S.T. (2010) Coevolution of hydrology and topography on a basalt landscape in the Oregon Cascade Range, USA. *Earth Surface Processes and Landforms*, 35(7), 803-816. Available from: <https://doi.org/10.1002/esp.1976>

Jones, M.W., Abatzoglou, J.T., Veraverbeke, S., Andela, N., Lasslop, G., Forkel, M., et al. (2022) Global and regional trends and drivers of fire under climate change. *Reviews of Geophysics*, 60(3), e2020RG000726. Available from: <https://doi.org/10.1029/2020RG000726>

Kean, J.W., Staley, D.M., Lancaster, J.T., Rengers, F.K., Swanson, B.J., Coe, J.A., et al. (2019) Inundation, flow dynamics, and damage in the 9 January 2018 Montecito debris-flow event, California, USA: opportunities and challenges for post-wildfire risk assessment. *Geosphere*, 15(4), 1140-1163. Available from: <https://doi.org/10.1130/GES02048.1>

Keller, E.A., Valentine, D.W. & Gibbs, D.R. (1997) Hydrological response of small watersheds following the Southern California painted cave fire of June 1990. *Hydrological Processes*, 11(4), 401-414. Available from: [https://doi.org/10.1002/\(sici\)1099-1085\(19970330\)11:4<401::aid-hyp447>3.0.co;2-p](https://doi.org/10.1002/(sici)1099-1085(19970330)11:4<401::aid-hyp447>3.0.co;2-p)

Littell, J.S., McKenzie, D., Wan, H.Y. & Cushman, S.A. (2018) Climate change and future wildfire in the western United States: an ecological approach to nonstationarity. *Earth's Future*, 6(8), 1097-1111. Available from: <https://doi.org/10.1029/2018EF000878>

Mao, L., Uyttendaele, G.P., Iroum  , A. & Lenzi, M.A. (2008) Field based analysis of sediment entrainment in two high gradient streams located in Alpine and Andine environments. *Geomorphology*, 93(3-4), 368-383. Available from: <https://doi.org/10.1016/j.geomorph.2007.03.008>

May, C.L. & Gresswell, R.E. (2004) Spatial and temporal patterns of debris-flow deposition in the Oregon coast range, USA. *Geomorphology*, 57(3-4), 135-149. Available from: [https://doi.org/10.1016/S0169-555X\(03\)00086-2](https://doi.org/10.1016/S0169-555X(03)00086-2)

May, C.L. & Lee, D.C. (2004) The relationships among in-channel sediment storage, pool depth, and summer survival of juvenile salmonids in Oregon coast range streams. *North American Journal of Fisheries Management*, 24(3), 761-774. Available from: <https://doi.org/10.1577/m03-073.1>

McGuire, L.A., Rengers, F.K., Kean, J.W., Staley, D.M. & Mirus, B.B. (2018) Incorporating spatially heterogeneous infiltration capacity into hydrologic models with applications for simulating post-wildfire debris flow initiation. *Hydrological Processes*, 32(9), 1173-1187. Available from: <https://doi.org/10.1002/hyp.11458>

McGuire, L.A., Rengers, F.K., Kean, J.W., Staley, D.M., Tang, H. & Youberg, A.M. (2019) Looking through the window of disturbance at post-wildfire debris flow hazards. In: Kean, J. W., Coe, J. A., Santi, P. M. & Guillen, B. K. (Eds.) *Debris-flow hazards mitigation: Mechanics, monitoring, modelling, and assessment* (pp. 516-523). Association of Environmental and Engineering Geologists, Colorado, United States. Special publication 28, 7th International Conference on Debris-Flow Hazards Mitigation.

McIver, J.D. & Starr, L. (2001) A literature review on the environmental effects of postfire logging. *Western Journal of Applied Forestry*, 16(4), 159-168. Available from: <https://doi.org/10.1093/wjaf/16.4.159>

McNabb, D. & Swanson, F. (1990) Effects of fire on soil erosion. *Journal of Range Management*, 43(5), 470. Available from: <https://doi.org/10.2307/4002670>

Minshall, G.W., Robinson, C.T. & Lawrence, D.E. (1997) Postfire responses of lotic ecosystems in Yellowstone National Park, U.S.A. *Canadian Journal of Fisheries and Aquatic Sciences*, 54(11), 2509-2525. Available from: <https://doi.org/10.1139/cjfas-54-11-2509>

Moffett, K.B. & Quinn, D. S. (2023) Prescribed fire effects on soil hydraulic properties and ecohydrological function, Joint Fire Science Program, Final report, JFSP Project 20-1-01-26.

Montgomery, D.R. & Buffington, J.M. (1998) Channel processes, classification, and response. In: Naiman, R.J. & Bilby, R.E. (Eds.), *River Ecology and Management: Lessons from the Pacific Coastal Ecoregion*, (pp.13-42), Springer, New York. New York. https://doi.org/10.1007/978-1-4612-1652-0_2

Montgomery, D.R., Collins, B.D., Buffington, J.M. & Abbe, T.B. (2003) Geomorphic effects of wood in rivers. *American Fisheries Society Symposium*, 37, 21-47.

Moody, J.A., Shakesby, R.A., Robichaud, P.R., Cannon, S.H. & Martin, D.A. (2013) Current research issues related to post-wildfire runoff and erosion processes. *Earth-Science Reviews*, 122, 10-37. Available from: <https://doi.org/10.1016/j.earscirev.2013.03.004>

O'Connor, J.E., Mangano, J.F., Anderson, S.W., Wallick, J.R., Jones, K.L. & Keith, M.K. (2014) Geologic and physiographic controls on bed-material yield, transport, and channel morphology for alluvial and bedrock rivers, western Oregon. *Geological Society of America Bulletin*, 126(3-4), 377-397. Available from: <https://doi.org/10.1130/B30831.1>

O'Neill, L., Hatchett, B. & Dalton, M. (2021) Drought. In: Dalton, M.M. & Fleishman, E. (Eds.) *Fifth Oregon climate assessment*. Corvallis, Oregon: Oregon Climate Change Research Institute, Oregon State University, pp. 37-45 https://ir.library.oregonstate.edu/concern/parent/pz50h457p/file_sets/tx31qs642, <https://doi.org/10.5399/osu/1160>

Pitlick, J. (1994) Relation between peak flows, precipitation, and physiography for five mountainous regions in the western USA. *Journal of Hydrology*, 158(3-4), 219-240. Available from: [https://doi.org/10.1016/0022-1694\(94\)90055-8](https://doi.org/10.1016/0022-1694(94)90055-8)

PRISM Climate Group. (2022). *30-year normal precipitation 1991-2020*, Oregon State University. Oregon, Oregon: Earth Surface Processes and Landforms. <https://prism.oregonstate.edu/normal/>

Raymond, C.A., McGuire, L.A., Youberg, A.M., Staley, D.M. & Kean, J.W. (2020) Thresholds for post-wildfire debris flows: Insights from the Pinal Fire, Arizona, USA. 45, 1349-1360 p. <https://doi.org/10.1002/esp.4805>

Recking, A. (2009) Theoretical development on the effects of changing flow hydraulics on incipient bed load motion. *Water Resources Research*, 45(4), 1-16. Available from: <https://doi.org/10.1029/2008WR006826>

Recking, A., Leduc, P., Li  ault, F. & Church, M. (2012) A field investigation of the influence of sediment supply on step-pool morphology and stability. *Geomorphology*, 139-140, 53-66. Available from: <https://doi.org/10.1016/j.geomorph.2011.09.024>

Reilly, M.J., Zuspan, A., Halofsky, J.S., Raymond, C., McEvoy, A., Dye, A.W., et al. (2022) Cascadia burning: the historic, but not historically unprecedented, 2020 wildfires in the Pacific northwest, USA. *Ecosphere*, 13(6), e4070. Available from: <https://doi.org/10.1002/ecs2.4070>

Rengers, F.K., McGuire, L.A., Barnhart, K.R., Youberg, A.M., Cadol, D., Gorr, A.N., et al. (2023) The influence of large woody debris on post-

wildfire debris flow sediment storage. *Natural Hazards and Earth System Sciences*, 23(6), 2075–2088. Available from: <https://doi.org/10.5194/nhess-23-2075-2023>

Rengers, F.K., McGuire, L.A., Oakley, N.S., Kean, J.W., Staley, D.M. & Tang, H. (2020) Landslides after wildfire: initiation, magnitude, and mobility. *Landslides*, 17(11), 2631–2641. Available from: <https://doi.org/10.1007/s10346-020-01506-3>

Robichaud, P.R. (2000) Fire effects on infiltration rates after prescribed fire in northern Rocky Mountain forests, USA. *Journal of Hydrology*, 231, 220–229. Available from: [https://doi.org/10.1016/S0022-1694\(00\)00196-7](https://doi.org/10.1016/S0022-1694(00)00196-7)

Roebuck, J.A., Jr., Bladon, K.D., Donahue, D., Graham, E.B., Grieger, S., Morgenstern, K., et al. (2022) Spatiotemporal controls on the delivery of dissolved organic matter to streams following a wildfire. *Geophysical Research Letters*, 49(16), e2022GL099535.

Roering, J.J. & Gerber, M. (2005) Fire and the evolution of steep, soil-mantled landscapes. *Geology*, 33(5), 349–352. Available from: <https://doi.org/10.1130/G21260.1>

Roering, J.J., Schmidt, K.M., Stock, J.D., Dietrich, W.E. & Montgomery, D.R. (2003) Shallow landsliding, root reinforcement, and the spatial distribution of trees in the Oregon coast range. *Canadian Geotechnical Journal*, 40(2), 237–253. Available from: <https://doi.org/10.1139/t02-113>

Shakesby, R.A. & Doerr, S.H. (2006) Wildfire as a hydrological and geomorphological agent. *Earth-Science Reviews*, 74(3–4), 269–307. Available from: <https://doi.org/10.1016/j.earscirev.2005.10.006>

Short, L.E., Gabet, E.J. & Hoffman, D.F. (2015) The role of large woody debris in modulating the dispersal of a post-fire sediment pulse. *Geomorphology*, 246, 351–358. Available from: <https://doi.org/10.1016/j.geomorph.2015.06.031>

Sickinger, T. (2022) PacifiCorp settles lawsuit with two families who were victims of Archie Creek fire in 2020, The Oregonian, 4 November, <https://www.oregonlive.com/wildfires/2022/11/pacificorp-settles-lawsuit-with-two-families-who-were-victims-of-archie-creek-fire-in-2020.html>

Sidle, R.C., Pearce, A.J., O'Loughlin, C.L. (1985) Hillslope stability and land use: American Geophysical Union Water Resource Monograph no. 11, 140 p, <https://doi.org/10.1029/WM011>

Staley, D.M., Negri, J.A., Kean, J.W., Laber, J.L., Tillery, A.C. & Youberg, A.M. (2017) Prediction of spatially explicit rainfall intensity-duration thresholds for post-fire debris-flow generation in the western United States. *Geomorphology*, 278, 149–162. Available from: <https://doi.org/10.1016/j.geomorph.2016.10.019>

Swanson, F.J. (1975) *Geology and geomorphology of the HJ Andrews Experimental Forest, Western Cascades, Oregon (no. 188-204)*. Pacific Northwest Forest and Range Experiment Station, Forest Service, US Department of Agriculture, Portland, Oregon.

Swanson, F.J. (1981) Fire and geomorphic processes. In: Mooney, H.A., Bonnicksen, T.M., Christiansen, N.L., Lotan, J.E. & Reiners, W.A. (Eds.) *Fire regime and ecosystem properties, United States Department of Agriculture, Forest Service, general technical report WO*, Vol. 26. Washington, DC: United States Government Planning Office, pp. 401–421.

Thomas, M.A., Lindsay, D.N., Cavagnaro, D.B., Kean, J.W., McCoy, S.W. & Gruber, A.P. (2023) The rainfall intensity-duration control of debris flows after wildfire. *Geophysical Research Letters*, 50(10), e2023GL103645.

Touma, D., Stevenson, S., Swain, D.L., Singh, D., Kalashnikov, D.A. & Huang, X. (2022) Climate change increases risk of extreme rainfall following wildfire in the western United States. *Science. Advances*, 8(13), eabm0320. Available from: <https://doi.org/10.1126/sciadv.abm0320>

U.S. Forest Service. (2022) *FSGeodata clearinghouse*. Department of Agriculture, <https://data.fs.usda.gov/geodata/>

U.S. Geological Survey. (2020) *Emergency assessment of post-fire debris-flow hazards*. Department of Interior, https://landslides.usgs.gov/hazards/postfire_debrisflow/

U.S. Geological Survey. (2022a) *Landscape fire and resource management planning tools (LANDFIRE)*. Department of Interior, <https://landfire.gov/index.php>

U.S. Geological Survey. (2022b) *StreamStats version 4*. Department of Interior, <https://streamstats.usgs.gov/ss/>

U.S. Geological Survey. (2024) National Water Information System, USGS 14317450 North Umpqua River near Idleyd Park, OR.

U.S. Geological Survey. and USFS (U.S. Forest Service). (2020) *BAER imagery support program*. Department of Interior and Department of Agriculture, <https://burnseverity.cr.usgs.gov/baer/>

U.S. Geological Survey. and USFS (U.S. Forest Service). (2022) *Monitoring trends in burn severity*. Department of Interior and Department of Agriculture, <https://www.mtbs.gov/>

Vieira, D.C.S., Fernández, C., Vega, J.A. & Keizer, J.J. (2015) Does soil burn severity affect the post-fire runoff and interrill erosion response? A review based on meta-analysis of field rainfall simulation data. *Journal of Hydrology*, 523, 452–464. Available from: <https://doi.org/10.1016/j.jhydrol.2015.01.071>

Welling, R.T., Wilcox, A.C. & Dixon, J.L. (2021) Large wood and sediment storage in a mixed bedrock-alluvial stream, western Montana, USA. *Geomorphology*, 384, 107703. Available from: <https://doi.org/10.1016/j.geomorph.2021.107703>

Wiley, T.J. (2000) Relationship between rainfall and debris flows in western Oregon. *Oregon Geology*, 62, 27–43.

Williams, A.P., Cook, B.I. & Smerdon, J.E. (2022) Rapid intensification of the emerging southwestern North American megadrought in 2020–2021. *Nature Climate Change*, 12(3), 232–234. Available from: <https://doi.org/10.1038/s41558-022-01290-z>

Wohl, E., Cenderelli, D.A., Dwire, K.A., Ryan-Burkett, S.E., Young, M.K. & Fausch, K.D. (2010) Large in-stream wood studies: a call for common metrics. *Earth Surface Processes and Landforms*, 35(5), 618–625. Available from: <https://doi.org/10.1002/esp.1966>

Wohl, E., Marshall, A.E., Scamardo, J., White, D. & Morrison, R.R. (2022) Biogeomorphic influences on river corridor resilience to wildfire disturbances in a mountain stream of the southern Rockies, USA. *Science of the Total Environment*, 820, 153321. Available from: <https://doi.org/10.1016/j.scitotenv.2022.153321>

Wolman, G.M. (1954) A method of sampling coarse river-bed material. *Transaction of the American Geophysical Union*, 35(6), 951–956. Available from: <https://doi.org/10.1029/TR035i006p00951>

Wondzell, S.M. & King, J.G. (2003) Postfire erosional processes in the Pacific northwest and Rocky Mountain regions. *Forest Ecology and Management*, 178(1–2), 75–87. Available from: [https://doi.org/10.1016/S0378-1127\(03\)00054-9](https://doi.org/10.1016/S0378-1127(03)00054-9)

Wood, P.J. & Armitage, P.D. (1997) Biological effects of fine sediment in the lotic environment. *Environmental Management*, 21(2), 203–217. Available from: <https://doi.org/10.1007/s002679900019>

How to cite this article: Busby, D.M. & Wilcox, A.C. (2024) Hydrogeomorphic response of steep streams following severe wildfire in the Western Cascades, Oregon. *Earth Surface Processes and Landforms*, 1–17. Available from: <https://doi.org/10.1002/esp.5982>